Journal of Magnetism and Magnetic Materials 380 (2015) 39–45

Contents lists available at ScienceDirect

Journal of Magnetism and Magnetic Materials

journal homepage: www.elsevier.com/locate/jmmm

Polyelectrolyte coating of ferumoxytol nanoparticles for labeling of dendritic cells

Nehar Celikkin [a,b,1], Lucie Jakubcová [a,b], Martin Zenke [a,b], Mareike Hoss [c], John Erik Wong [d,e,*], Thomas Hieronymus [a,b,**]

[a] Institute for Biomedical Engineering, Department of Cell Biology, RWTH Aachen University Hospital, Pauwelsstrasse 30, 52074 Aachen, Germany
[b] Helmholtz Institute for Biomedical Engineering, RWTH Aachen University, Pauwelsstrasse 20, 52074 Aachen, Germany
[c] Institute of Pathology, Electron Microscopy Facility, RWTH Aachen University Hospital, Pauwelsstrasse 30, 52074 Aachen, Germany
[d] Chemical Process Engineering, RWTH Aachen University, Turmstrasse 46, 52056 Aachen, Germany
[e] DWI – Leibniz Institute for Interactive Materials Research, Forckenbeckstrasse 50, Aachen, Germany

ARTICLE INFO

Article history:
Received 30 June 2014
Received in revised form
29 August 2014
Accepted 2 September 2014
Available online 10 September 2014

Keywords:
Nanoparticles
Ferumoxytol
Polyelectrolytes
Layer-by-Layer technique
Dendritic cell tracking

ABSTRACT

Engineered magnetic nanoparticles (MNPs) are emerging to be used as cell tracers, drug delivery vehicles, and contrast agents for magnetic resonance imaging (MRI) for enhanced theragnostic applications in biomedicine. In vitro labeling of target cell populations with MNPs and their implantation into animal models and patients shows promising outcomes in monitoring successful cell engraftment, differentiation and migration by using MRI. Dendritic cells (DCs) are professional antigen-presenting cells that initiate adaptive immune responses. Thus, DCs have been the focus of cellular immunotherapy and are increasingly applied in clinical trials. Here, we addressed the coating of different polyelectrolytes (PE) around ferumoxytol particles using the layer-by-layer technique. The impact of PE-coated ferumoxytol particles for labeling of DCs and $Flt3^+$ DC progenitors was then investigated. The results from our studies revealed that PE-coated ferumoxytol particles can be readily employed for labeling of DC and DC progenitors and thus are potentially suitable as contrast agents for MRI tracking.

1. Introduction

Magnetic materials play important roles in the development of modern technologies including the recently investigated high potential of magnetic nanoparticles (MNPs) [1]. MNPs are used in biomedicine for cell tracking [2–4], drug delivery [1,5] and as contrast agent for magnetic resonance imaging (MRI) [6]. Using MNPs in cell tracking is one of the most attractive applications due to recent progress in cellular therapies. Monitoring of the initial engraftment, distribution pattern, and/or migration of transplanted cells to the pathological site remains crucial for the success of such therapies.

Dendritic cells (DCs) are professional antigen-presenting cells that initiate adaptive immune responses. By controlling DC function, the immune response of the patient can be altered or adjusted. Such therapies represent attractive means for the treatment of tumors or autoimmune diseases and to prevent organ rejection after transplantations [7]. Thus, DCs are increasingly employed as cellular vaccines in clinical trials [8]. Due to their phagocytic capacity DCs have been successfully labeled with MNPs and tracked using MRI [2].

Ferumoxytol is an FDA and EMA approved drug based on an iron-oxide nanoparticle formulation and used in iron-deficiency anemia in chronic kidney disease [9]. In previous studies, ferumoxytol has been used as a macrophage-imaging agent as well as a blood-pool agent with MRI [9–11]. However, ferumoxytol alone did not result in effective cell labeling [12].

Surface modification of MNPs with biocompatible materials increases the stability of these particles, while in the absence of any surface coating the hydrophobic interactions between the particles causes agglomeration that can lead to insoluble precipitates [13]. In previous studies, the Layer-by-Layer (LbL) technique was successfully applied for modifying the surface of MNPs [2,14–16]. LbL

Abbreviations: DCs, Dendritic cells; LbL, Layer-by-Layer; MNPs, magnetic nanoparticles; MRI, magnetic resonance imaging; PDADMAC, polydiallyldimethylammonium chloride; PEI, polyethyleneimine; PE, polyelectrolyte

* Corresponding author at: Chemical Process Engineering (AVT.CVT), RWTH Aachen University, Turmstr. 46, 52056 Aachen, Germany. Tel.: +49 241 80 29945; fax: +49 241 80 92252.

** Corresponding author at: Institute for Biomedical Engineering, Department of Cell Biology, RWTH Aachen University Hospital, Pauwelsstrasse 30, 52074 Aachen, Germany. Tel.: +49 241 80 85249; fax: +49 241 80 82008.

E-mail addresses: John.Wong@avt.rwth-aachen.de (J.E. Wong), thomas.hieronymus@rwth-aachen.de (T. Hieronymus).

[1] present address: Faculty of Materials Science and Engineering, Warsaw University of Technology, IPPT PAN, Pawinskiego Street 5B; 02-106 Warsaw, Poland

http://dx.doi.org/10.1016/j.jmmm.2014.09.001
0304-8853/

assembly involves the sequential adsorption of polyelectrolytes (PE) on a charged substrate. LbL assembly is an easy, versatile, and generic technique for surface modification, particularly on the nanometer scale. The thickness of each PE layer and thus of the entire film, and the morphology, can be monitored and tuned by varying the ionic strength, type of salts, pH and temperature of the solutions from which these layers are fabricated. These multilayered materials and structures can be optimized with specific properties such as optical, magnetic, or electrical [17–19].

Our main objectives for this study were establishing the PE-coating of ferumoxytol using LbL assembly and labeling of DCs with PE-modified ferumoxytol for MRI tracking. Furthermore, we investigated the impact of PE coating on cell viability, labeling efficiency and intracellular iron content of cells at different states of DC differentiation including Flt3$^+$ progenitors and terminally differentiated DCs.

2. Materials and Methods

2.1. LbL assembly of polyelectrolytes on ferumoxytol

The FDA and EMA approved iron-oxide nanoparticle formulation ferumoxytol (Rienso®) was purchased from Takeda Pharma. High molecular weight (MW) polyethyleneimine (PEI, 750 kDa), low MW PEI (25 kDa), high MW polydiallyldimethylammonium chloride (PDADMAC, 400–500 kDa) and low MW PDADMAC (100–200 kDa) were obtained from Sigma-Aldrich. The surface coating of ferumoxytol was carried out in double distilled water using the LbL technique to deposit polyelectrolyte layers [5,14,20]. The negatively charged ferumoxytol MNPs were added to an aqueous solution of the positively charged polyelectrolytes to prepare the first layer. The solutions were incubated for 24 h to ensure that saturation adsorption of the polyions on the colloid particles was reached. The products were separated from the excess polyelectrolyte by magnetic separation and rinsed with water twice to remove any loosely bound PE. The hydrodynamic size of the MNPs was obtained from dynamic light scattering by cumulant fits using a Zetasizer 3000HSA (Malvern Instruments), which also provides the zeta potentials (ζ-potential) of the particles; each value reported is an average of at least ten consistent measurements performed in water. The particles were visualized by transmission electron microscopy (TEM) and TEM images analyzed using ImageJ. Thermogravimetric analysis (TGA) was carried out on the dried samples with a heating rate of 10 °C/min (from 20 °C to 950 °C), using a DuPont 9900 thermogravimetric analyzer in a nitrogen atmosphere.

2.2. DC culture and phenotypic characterization

DCs were differentiated from hematopoietic Flt3$^+$ precursor cells of bone marrow suspensions from C57BL/6 mice (Charles River) as described [21]. In brief, Flt3$^+$ DC progenitors were obtained from bone marrow cells after 7 days of proliferation in RPMI 1640 medium supplemented with 10% FCS, 2 mM L-glutamine, 100 U/ml penicillin/streptomycin, and 50 μM β-mercaptoethanol (all from Invitrogen) containing recombinant murine SCF (100 ng/ml), 25 ng/ml Flt3-ligand (PeproTech), 40 ng/ml recombinant long-range IGF-1 (Sigma-Aldrich), 5 ng/ml hyper IL-6, 20 U/ml recombinant mouse GM-CSF, and 10^{-6} M dexamethasone (Sigma-Aldrich). After 7 days, differentiation of Flt3$^+$ progenitors into DCs was induced in culture medium

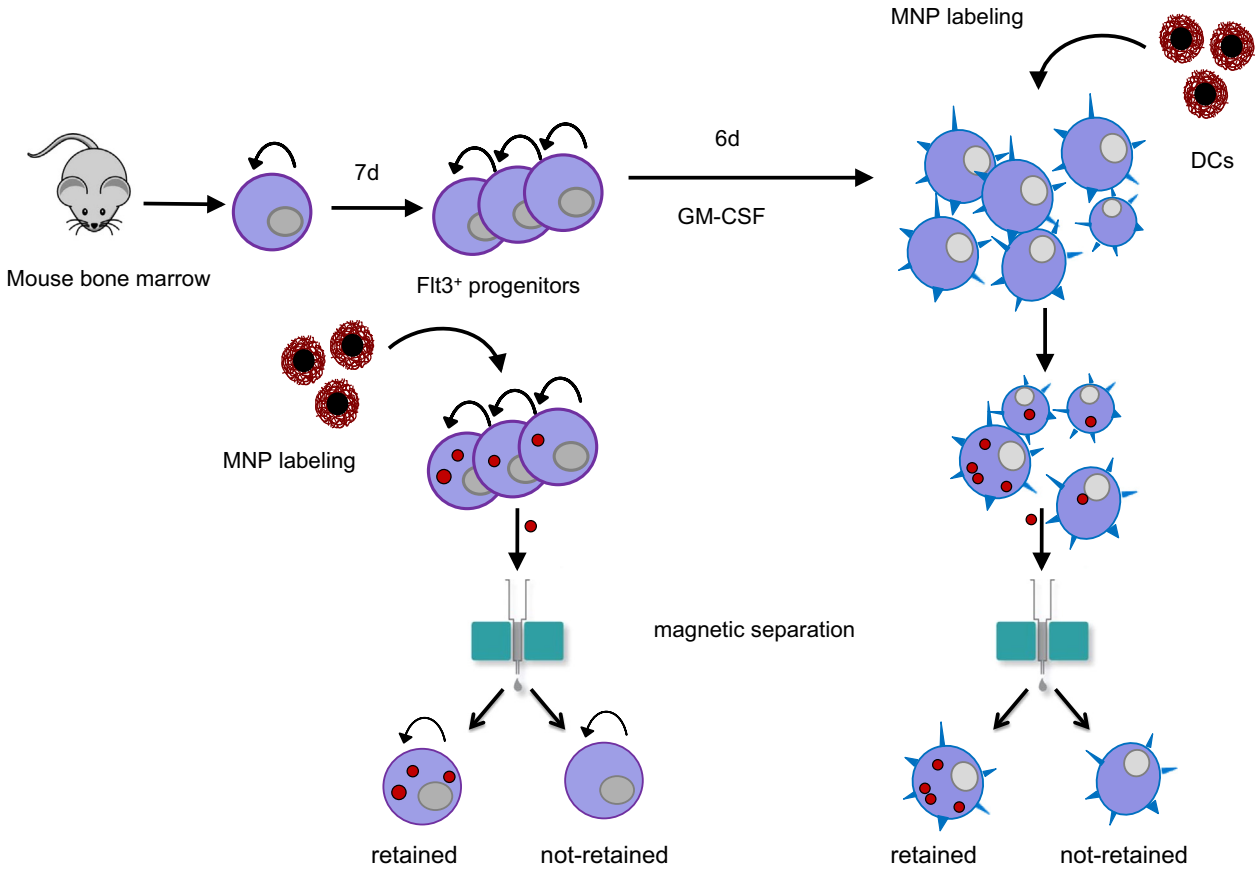

Fig. 1. Schematic representation of the 2-step culture system for differentiation of DCs from Flt3$^+$ progenitors and magnetic separation following labeling with PE-coated MNPs.

supplemented with 200 U/ml recombinant murine GM-CSF. Fully differentiated immature DCs obtained after 6 days of differentiation were used to investigate DC-MNP interaction (Fig. 1). Cell numbers were determined with an electronic cell counting device (CASY1, Schaerfe System). Flow cytometry analysis was used to determine the phenotype of $Flt3^+$ progenitors and DCs prior to and after MNP-labeling as previously described [14,21]. Mice were maintained under specific pathogen free conditions in the central animal facility of the RWTH University Hospital Aachen. All animal experiments were approved by local authorities (Bezirksregierung Köln) in compliance with the German animal protection law.

2.3. MNP-labeling of DCs

Sterile solutions of ferumoxytol MNPs were sonicated for 30 min prior to cell labeling and used with a final iron concentration of 10 μg/ml in cell culture medium. DCs were seeded at 2×10^6 cells/ml and incubated with MNPs for 24 h. Cells were harvested and washed in a PBS solution containing 2% FCS before being subjected to magnetic separation (MACS, Miltenyi Biotech) as previously reported [2,14]. The labeling efficiency was calculated by counting the retained cells after the magnetic separation (Eq.1). Retained and not-retained cell numbers were determined using CASY1 cell counter.

Labeling efficiency (%)=Retained Cell Number/Total Cell Number x 100 (Eq. 1)

2.4. Cell viability assessment after MNP-labeling

Cytotoxicity of PE-coated and uncoated MNPs on DCs and $Flt3^+$ progenitors was evaluated using the Zombie Aqua Viability Kit (BioLegend) according to manufacturer' s protocol. Briefly, 5×10^5 cells after MNP-labeling were incubated in a 1:100 (v/v) dilution of the Zombie Aqua dye in a total volume of 50 μl PBS for 20 min at room temperature in the dark. After washing with PBS, cells were analyzed with a FACSCanto II flow cytometer (BD Biosciences) and data were evaluated using FlowJo software (Miltenyi Biotech).

2.5. Quantification of cellular iron content

Intracellular iron concentration was determined using colorimetric ferrozine iron assay as previously described [2,14]. Briefly, 1×10^6 DCs were lysed in 100 μl 50 mM NaOH and ascorbic acid was used to reduce Fe^{3+} to Fe^{2+} ions that form a chelate complex with ferrozine (3-(2-pyridyl)-5,6-bis(phenyl sulfonic acid)-1,2,4-triazine; Sigma-Aldrich). Absorbance of Fe^{2+}-ferrozine was measured at 550 nm using a FLUOStar OPTIMA plate reader (BMG Labtech) and compared to the absorbance of $FeCl_3$ standards.

2.6. Prussian blue staining of intracellular iron

To visualize the total iron uptake of cells, 1×10^5 cells labeled with MNPs were centrifuged (7 min at 700 rpm) onto a glass slide using a cytospin centrifuge (Thermo Fisher Scientific). After washing in double-distilled (dd) H_2O, glass slides were subjected to Prussian Blue staining using a 1:1 solution (v/v) of 10% $K_4[Fe(CN)_6]$ (Sigma-Aldrich) and 20% HCl for 20 min. After washing in ddH_2O, glass slides were counter-stained with Neutral Red dye (Roth) and mounted with cover slips using mounting medium (Dako). Sample images were obtained using Leica DM6000B microscope and Diskus acquisition software (Hilgers).

2.7. Transmission electron microscopy

Transmission electron microscopy (TEM) images were obtained from 1×10^6 magnetically sorted DCs. Cells were fixed with 3% (w/v) glutaraldehyde and embedded in 2% agarose. Samples were stained with OsO_4, embedded in Epon and cut into 70 nm thick slices. Samples were analyzed without further contrast enhancement using a Philips EM 400 T electron microscope at 60 kV equipped with a CCD camera (MORADA, Olympus). TEM images were analyzed using ImageJ.

2.8. Statistical analysis

Uptake of MNPs by cells and intracellular iron contents are expressed as mean values ± standard deviation (SD). Numerical data were analyzed for significance by Student's t test with GraphPad Prism software. A p value below 0.05 was considered significant.

3. Results and discussion

3.1. Ferumoxytol coating with polyelectrolyes and particle characterization

The MNP shell is a critical constituent to provide colloidal stability and to impart biocompatibility [13,22]. Accordingly, the MNP shell has been shown to play a major impact on cellular responses, including cell viability as well as uptake, intracellular localization, and processing of MNPs, and thus on contrast agent properties for cell tracking using MRI. Therefore, MNP shells are frequently tailored to improve cell targeting including coating with PE. In previous studies, ferumoxytol particles have shown inefficient cell labeling [12].

In this study, we therefore modified ferumoxytol particles with high and low MW polyethyleneimine (PEI), and with high and low MW polydiallyldimethylammoniumchloride (PDADMAC) using the Layer-by-Layer (LbL) assembly [14]. Different amounts of ferumoxytol particles (3, 6, 9, 12 and 18 mg) were added into polyelectrolyte solutions with concentrations of 1 g/L or 2 g/L to find the optimum conditions for the LbL assembly of PE on ferumoxytol particles. PE-coated ferumoxytol particles were characterized for their hydrodynamic size (Supplementary Fig. S1) and surface charge as summarized in Table 1.

Ferumoxytol consists of an iron-oxide core with a core size of ~6 nm and a polyglucose sorbitol carboxymethylether (PSC) shell [11]. We determined a hydrodynamic diameter of 29 nm, in line with previously published results and a ζ-potential of −44 mV.

Upon LbL assembly of PE, a positive surface charge was measured that is indicative of successful coating with positively charged PE around the ferumoxytol particles. Furthermore the magnitude of the ζ-potential revealed that stable, coated particles were achieved [23].

As expected, for identical PE concentrations, a higher hydrodynamic size for high MW PE coated particles was observed than for those particles coated with low MW PE. The longer PE chains led to thicker coating layers around the ferumoxytol particles. Low MW PDADMAC coating around the ferumoxytol particles required optimization in particle and PE coating concentration due to difficulties in the magnetic separation. When the ferumoxytol particles were coated with the low MW PDADMAC concentration of 1 g/L, only a small portion of the suspended particles could be collected. For the big fraction of the particles, the magnetic and gravity forces were not strong enough to exceed the buoyancy forces. Thus, the concentration of low MW PDADMAC was increased to 2 g/L. This increase in PE concentration resulted in more entanglement of the PE chains forming the shell around ferumoxytol particles, leading to PDADMAC-coated MNPs with not only bigger shell (and thus a larger hydrodynamic size) but also to increasing load of ferumoxytol particles (Fig. 2). We observed the sum of the magnetic and gravity forces exceeded the buoyancy

Table 1
Physicochemical properties of LbL-modified and uncoated ferumoxytol particles.

Polyelectrolyte coating	Polyelectrolyte concentration (g/L)	Amount of ferumoxytol (mg)	Surface charge (mV)	Hydrodynamic diameter (nm)
uncoated ferumoxytol	–[b]	–[b]	−44	29
low MW PDADMAC	1	6	+45	560
low MW PDADMAC	1	9	+27	451
low MW PDADMAC[a]	2	9	+39	822
low MW PDADMAC	2	12	+51	851
high MW PDADMAC	1	9	+45	609
high MW PDADMAC	1	12	+43	–[c]
low MW PEI	1	3	+32	85
high MW PEI[a]	1	3	+44	808

[a] used for further cell labeling studies.
[b] not applicable.
[c] agglomeration of particles.

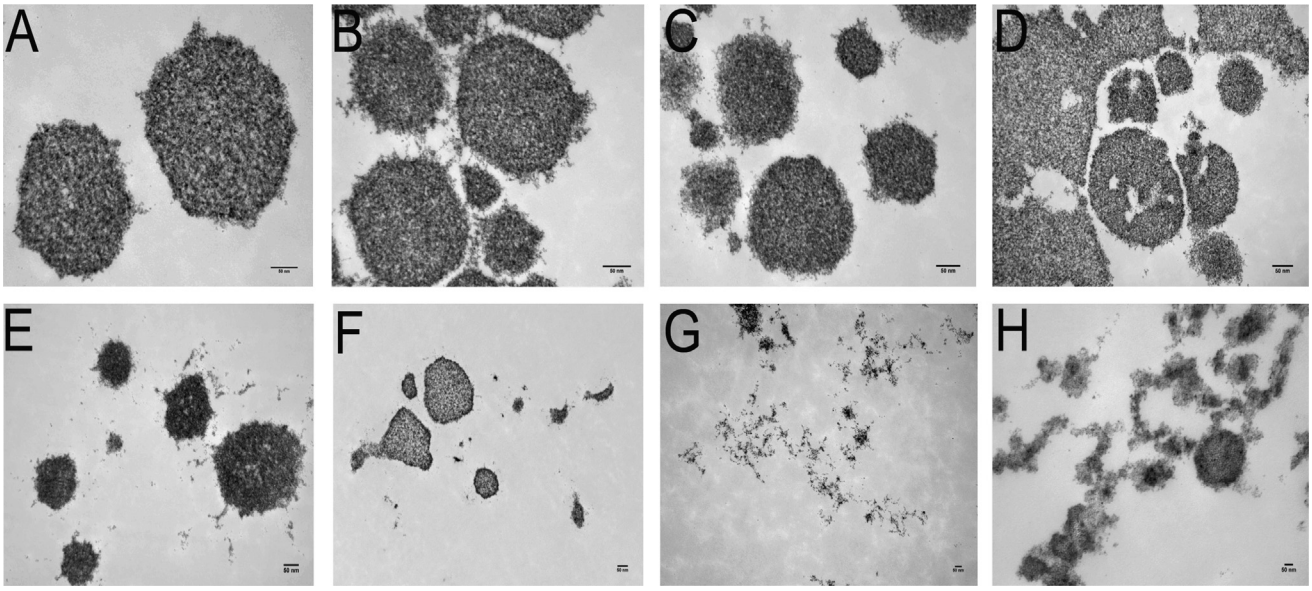

Fig. 2. TEM images of the PE-coated particles. (A) 6 mg ferumoxytol coated with low MW PDADMAC (1 g/L), (B) 9 mg ferumoxytol coated with low MW PDADMAC (1 g/L), (C) 9 mg ferumoxytol coated with low MW PDADMAC (2 g/L), (D) 12 mg ferumoxytol coated with low MW PDADMAC (2 g/L), (E) 9 mg ferumoxytol coated with high MW PDADMAC (1 g/L), (F) 12 mg ferumoxytol coated with high MW PDADMAC (1 g/L), (G) 3 mg ferumoxytol coated with low MW PEI (1 g/L), and (H) 3 mg ferumoxytol coated with high MW PEI (1 g/L). Scale bars, 50 nm.

forces for a larger fraction of these particles, facilitating separation and collection. In contrast, increasing the concentration of ferumoxytol particles to 12 mg or 18 mg resulted in large aggregates or insoluble precipitates. In the case of PEI-coating we observed for all combinations with ferumoxytol concentrations above 3 mg/ml only non-dispersible precipitates and only the colloidal stable PEI-coated particles were subjected to further analysis.

PE-coated ferumoxytol particles were analyzed by TEM and TEM images revealed that ferumoxytol aggregated upon PE-coating to larger size clusters. The size of these clustered cores of PE-coated particles was analyzed using ImageJ and was determined to range between mean values of 56 to 210 nm.

Coating by PE was also quantified by TGA, and Fig. 3 shows the TGA curve for PEI- and PDADMAC-coated ferumoxytol. The initial weight losses up to about 200 °C is due to the loss of residual water in the samples. Above that temperature the pronounced weight loss up to 600 °C which appears to take place in two stages is due to the thermal degradation of the polyelectrolytes [24] and the PSC shell of ferumoxytol [25–27]. The TGA results confirm that the polyelectrolytes are indeed bound to the MNP.

3.2. Cell labeling studies using PE-coated ferumoxytol

Nanoparticles obtained from coating of ferumoxytol with low MW PDADMAC (2 g/L polyelectrolyte solution plus 9 mg ferumoxyol) or high MW PEI were identified to be most similar in size (hydrodynamic diameter) and surface charge and therefore used for further cell-labeling studies. In these studies, DCs and Flt3$^+$ progenitors were labeled with uncoated ferumoxytol, low MW PDADMAC-coated ferumoxytol particles (referred in the following as ferumoxytol+PDADMAC) and high MW PEI-coated ferumoyxtol particles (referred in the following as ferumoxytol+PEI).

After incubating the cells with the different particles, the cells were subjected to magnetic sorting to separate MNP-labeled and unlabeled cells and thus to quantify the efficiency of MNP uptake (Fig. 1). The labeling efficiency was calculated with the formula given in Eq. 1 and the results are shown in Fig. 4.

DCs showed significantly higher labeling efficiency than Flt3$^+$ progenitors regardless of the particle coating, in line with previous studies using lipid-shell coated MNPs [2]. This may be due to their exceptional phagocytic capacity and indeed, phagocytosis

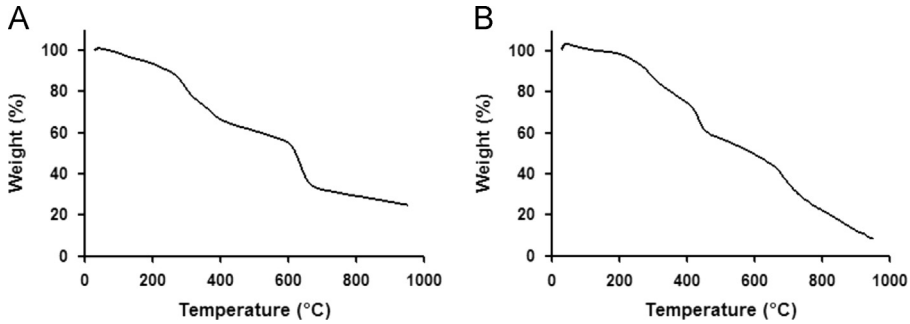

Fig. 3. TGA curve showing % of weight loss of thermal decomposition of PEI-coated MNPs (A) and PDADMAC-coated MNPs (B).

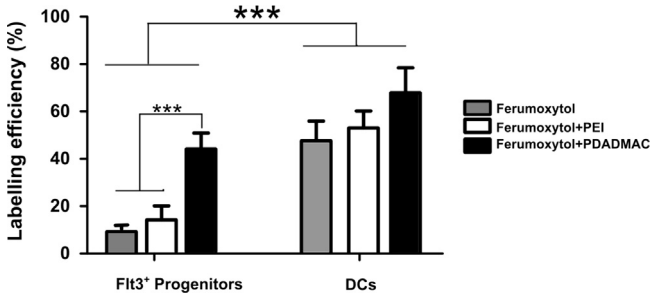

Fig. 4. Labeling efficiency of PE-coated and uncoated ferumoxytol particles taken up by cells as measured by magnetic separation. Results are mean values ± SD ($n=3$; ***: $p<0.01$).

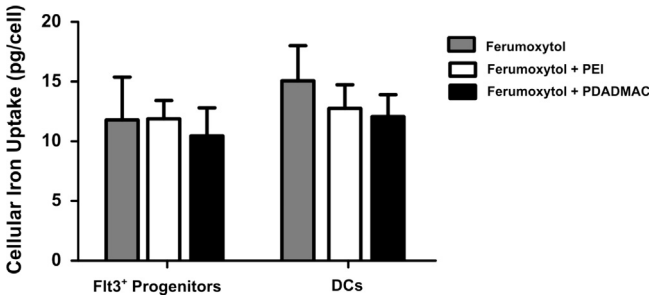

Fig. 5. Colorimetric iron assay displaying amount of intracellular iron. Graphs show mean values ± SD from three independent experiments.

was revealed as one of the major uptake mechanisms for large PE-coated particles [28]. However, MNP-coating using PDADMAC improved MNP take up by cells. This was most evident for labeling of Flt3$^+$ progenitors where PDADMAC-coated ferumoxytol was taken up by around 50% of cells compared to 10% and 15% of cells labeled with ferumoxytol alone or with PEI-coated ferumoxytol, respectively. Interestingly, theses results show that the improved labeling capacity of PDADMAC-coated ferumoxytol cannot be attributed to the positive surface charge.

To examine whether MNPs affect cell viability of DCs or Flt3+ progenitors after MNP-uptake, MNP-labeled and unlabeled cells were subjected to Zombie Aqua staining for detection of dead cells. Unlabeled control cells showed a contingent of 4.6% and 3.2% of dead DCs and Flt3+ progenitors cells, respectively. After labeling with ferumoxytol 3.4% of DCs and 4.4% of Flt3+ progenitor cells were found dead. For DCs and Flt3+ progenitor cells labeled with PEI-coated MNPs the percentage of dead cells was found to be 3.9% and 3.1%, respectively. Cells labeled with PDADMAC-coated MNPs showed 2.3% and 2.0% of dead DCs and Flt3+ progenitors, respectively. Thus, labeling of DCs and Flt3+ progenitors using PE-coated and uncoated ferumoxytol particles did not result in adverse cytotoxic effects at least at the concentration used here for labeling and in agreement to previously published results [14]. Interestingly, particles size and surface charge revealed no impact on cytotoxicity in line with results from our previous study [14].

To quantify the amount of intracellular MNP after labeling a ferrozine-based colorimetric assay was applied that allows determining the average iron load of MNP-labeled cell. It was found that Flt3$^+$ progenitors were capable of taking up 11.8 ± 3.6 pg iron/cell with ferumoxytol particles, 11.9 ± 1.5 pg iron/cell with PEI-coated ferumoxytol particles, and 10.5 ± 2.3 pg iron/cell with PDADMAC-coated ferumoxytol particles. The iron concentrations in DCs were 15 ± 5.3 pg iron/cell with ferumoxytol particles, 12.8 ± 1.5 pg iron/cell with PEI-coated ferumoxytol particles, 12 ± 1.8 pg iron/cell with PDADMAC-coated ferumoxytol particles. The comparison of the results between Flt3$^+$ progenitors and DCs is shown in Fig. 5. No significant differences in the iron concentrations were observed for both cell types indicating that saturation of intracellular iron concentration was achieved.

Intracellular iron loading was visualized using Prussian blue staining that confirmed uptake of MNPs in labeled cells (Fig. 6). Iron deposits stained by Prussian blue showed internalized MNPs in retained cells and indicated variable distribution and/or clustering of the different MNPs. Prussian blue showed no staining in not-retained cells, confirming the absence of MNPs.

For further examination of intracellular localization and distribution of the MNPs, TEM images were taken (Fig. 7). Internalized MNPs were found to be localized in vesicles in the cytosol, but not in the nucleus. PE-coated MNPs showed a more dense agglomeration within subcellular compartments than uncoated ferumoxytol in both Flt3$^+$ progenitors and DCs. However, in DCs larger aggregates of PE-coated MNPs were observed. This is an important finding, since it was found that not only the intracellular iron concentration but also the intracellular distribution of MNPs has a significant impact on MRI contrast agent properties [14,29].

4. Conclusion

Our results identified the molecular weight of PE as a critical parameter to influence particle size (hydrodynamic diameter) and thus to shape morphology of ferumoxytol MNPs. The concentration of the PE solution showed a minor influence on particle morphology. The coating with PDADMAC revealed that with increased concentration of PE larger particle hydrodynamic sizes were observed. However, the concentration of the PE solution had no significant effect on the surface charge when the amount of ferumoxytol particles was kept between 6–12 mg and we found no influence on the size of the particle core clusters.

In our in vitro labeling studies we observed no adverse cytotoxic effects of both uncoated and PE-coated MNPs. The labeling efficiency

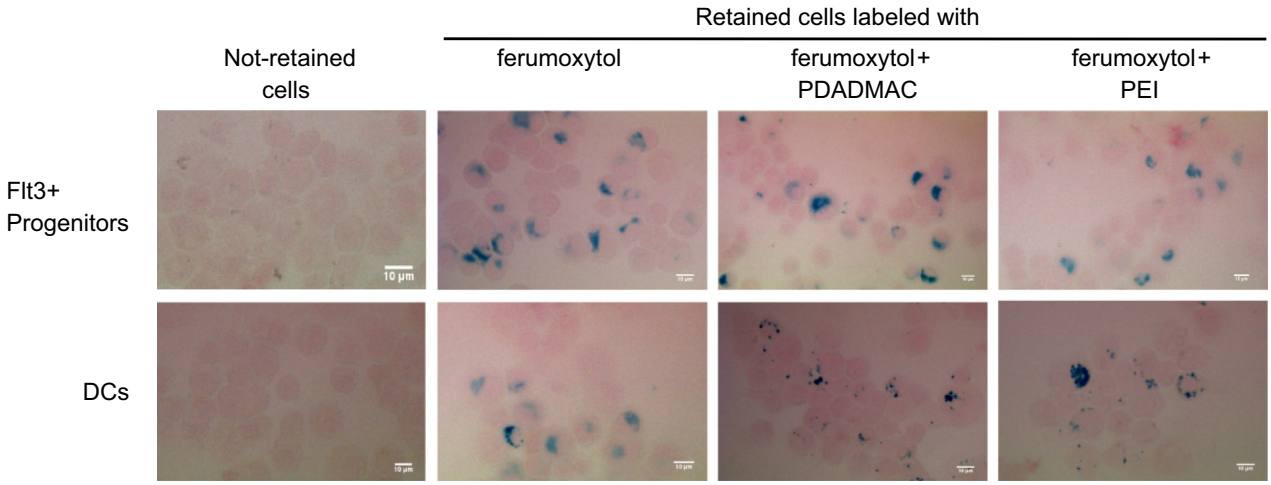

Fig. 6. Prussian blue staining of iron deposits. Cytospins of magnetically retained and not-retained cells were stained with Prussian blue for iron detection. Neutral red dye was used as counterstain. Scale bars, 10 μm.

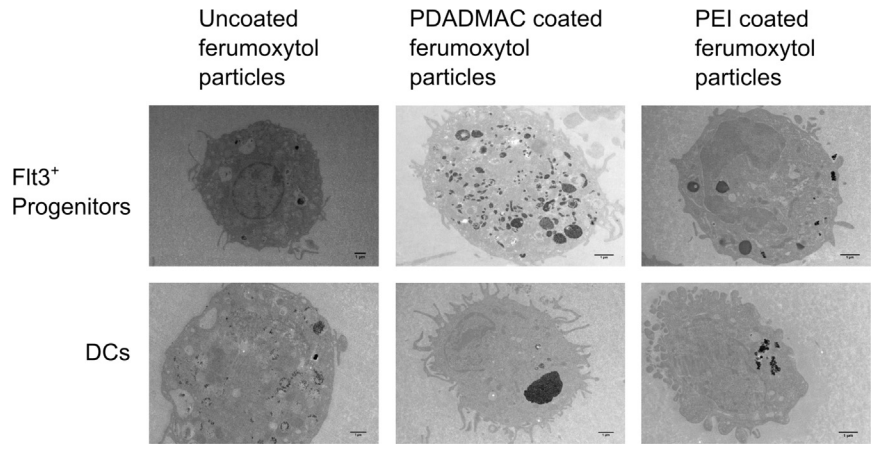

Fig. 7. Transmission electron micrographs of MNP-labeled cells. Scale bars, 1 μm.

was significantly higher when PE-coated ferumoxytol particles were used for both Flt3+ progenitors and DCs. Additionally, PE-coating of ferumoxytol resulted in a denser agglomeration within cells that will influence contrast agent properties in MRI. Taken together, we have demonstrated that PE-coating of ferumoxytol particles is feasible and can be used to tailor particle properties. Morevover, PE-coating of ferumoxytol particles impacts on the uptake by cells and revealed to be potentially suited as a label for DCs and DC progenitors for cell tracking using MRI.

Acknowledgments

We would like to thank H. Koenigs, RWTH Aachen University Hospital, Department of Pathology for assistance with electron microscopy. Part of this work was supported by the Excellence Initiative of the German federal and state governments (ERS OPSP006 to J. E. W. and T. H.) by RWTH Aachen University, Germany. T. H. received a grant from the START program of the Faculty of Medicine, RWTH Aachen University. N. C. thanks the CEMACUBE program (Erasmus Mundus, Action 1, Common European Master's course in Biomedical Engineering) for providing the scholarship.

Appendix A. Supporting information

Supplementary data associated with this article can be found in the online version at http://dx.doi.org/10.1016/j.jmmm.2014.09.001.

References

[1] M. Colombo, S. Carregal-Romero, M.F. Casula, L. Gutiérrez, M.P. Morales, I.B. Böhm, et al., Biological applications of magnetic nanoparticles, Chem Soc Rev 41 (2012) 4306–4334.
[2] S. Schwarz, F. Fernandes, L. Sanroman, M. Hodenius, C. Lang, U. Himmelreich, et al., Synthetic and biogenic magnetite nanoparticles for tracking of stem cells and dendritic cells, J Magn Magn Mater 321 (2009) 1533–1538.
[3] H.E. Daldrup-Link, R. Meier, M. Rudelius, G. Piontek, M. Piert, S. Metz, et al., In vivo tracking of genetically engineered, anti-HER2/neu directed natural killer cells to HER2/neu positive mammary tumors with magnetic resonance imaging, Eur Radiol 15 (2005) 4–13.
[4] J.W.M. Bulte, In vivo MRI cell tracking: clinical studies, AJR Am J Roentgenol 193 (2009) 314–325.
[5] J.E. Wong, A.K. Gaharwar, D. Müller-Schulte, D. Bahadur, W. Richtering, Layer-by-layer assembly of a magnetic nanoparticle shell on a thermoresponsive microgel core, J Magn Magn Mater 311 (2007) 219–223.
[6] Y-XJ. Wang, Superparamagnetic iron oxide based MRI contrast agents: Current status of clinical application, Quant Imaging Med Surg 1 (2011) 35–40.
[7] R.M. Steinman, J. Banchereau, Taking dendritic cells into medicine, Nature 449 (2007) 419–426.

[8] L. Galluzzi, L. Senovilla, E. Vacchelli, A. Eggermont, W.H. Fridman, J. Galon, et al., Trial watch: Dendritic cell-based interventions for cancer therapy, Oncoimmunology 1 (2012) 1111.
[9] M. Lu, M.H. Cohen, D. Rieves, R. Pazdur, FDA report: Ferumoxytol for intravenous iron therapy in adult patients with chronic kidney disease, Am J Hematol 85 (2010) 315–319.
[10] T. Christen, W. Ni, D. Qiu, H. Schmiedeskamp, R. Bammer, M. Moseley, et al., High-resolution cerebral blood volume imaging in humans using the blood pool contrast agent ferumoxytol, Magn Reson Med 70 (2013) 705–710.
[11] W. Li, S. Tutton, A.T. Vu, L. Pierchala, B.S.Y. Li, J.M. Lewis, et al., First-pass contrast-enhanced magnetic resonance angiography in humans using ferumoxytol, a novel ultrasmall superparamagnetic iron oxide (USPIO)-based blood pool agent, J Magn Reson Imaging 21 (2005) 46–52.
[12] M.S. Thu, L.H. Bryant, T. Coppola, E.K. Jordan, M.D. Budde, B.K. Lewis, et al., Self-assembling nanocomplexes by combining ferumoxytol, heparin and protamine for cell tracking by magnetic resonance imaging, Nat Med 18 (2012) 463–467.
[13] A.K. Gupta, M. Gupta, Synthesis and surface engineering of iron oxide nanoparticles for biomedical applications, Biomaterials 26 (2005) 3995–4021.
[14] S. Schwarz, J.E. Wong, J. Bornemann, M. Hodenius, U. Himmelreich, W. Richtering, et al., Polyelectrolyte coating of iron oxide nanoparticles for MRI-based cell tracking, Nanomedicine-Nanotechnology, Biology and Medicine 8 (2012) 682–691.
[15] M.-L. De Temmerman, S.J. Soenen, N. Symens, B. Lucas, R.E. Vandenbroucke, C. Libert, et al., Magnetic layer-by-layer coated particles for efficient MRI of dendritic cells and mesenchymal stem cells, Nanomedicine (from Future Medicine Ltd., UK) 20 (2013) 1–12.
[16] G. Liu, Z. Wang, H. Ai, J. Lu, C. Xia, F. Gao, et al., Low molecular weight alkyl-polycation wrapped magnetite nanoparticle clusters as MRI probes for stem cell labeling and in vivo imaging, Biomaterials 32 (2011) 528–537.
[17] G.B. Alcantara, L.G. Paterno, F.J. Fonseca, P.C. Morais, M.a.G. Soler, Morphology of cobalt ferrite nanoparticle–polyelectrolyte multilayered nanocomposites, J Magn Magn Mater 323 (2011) 1372–1377.
[18] J. Wong, W. Richtering, Layer-by-layer assembly on stimuli-responsive microgels, Curr Opin Colloid Interface Sci 13 (2008) 403–412.
[19] J.E. Wong, A.K. Gaharwar, D. Müller-Schulte, D. Bahadur, W. Richtering, Dual-stimuli responsive PNiPAM microgel achieved via layer-by-layer assembly: magnetic and thermoresponsive, J Colloid Interface Sci 324 (2008) 47–54.
[20] J.E. Wong, Surface Modification of Thermoresponsive Microgels via Layer-by-Layer Assembly of Polyelectrolyte Multilayers, Progr Colloid Polym Sci (2006) 45–51.
[21] T. Hieronymus, T.C. Gust, R.D. Kirsch, T. Jorgas, G. Blendinger, M. Goncharenko, et al., Progressive and Controlled Development of Mouse Dendritic Cells from Flt3+CD11b+ Progenitors In Vitro, J Immunol 174 (2005) 2552–2562.
[22] P. Rivera-Gil, D. Jimenez de Aberasturi, V. Wulf, B. Pelaz, P. del Pino, Y. Zhao, et al., The challenge to relate the physicochemical properties of colloidal nanoparticles to their cytotoxicity, Acc Chem Res 46 (2013) 743–749.
[23] V. Ayala, A.P. Herrera, M. Latorre-Esteves, M. Torres-Lugo, C. Rinaldi, Effect of surface charge on the colloidal stability and in vitro uptake of carboxymethyl dextran-coated iron oxide nanoparticles, J Nanopart Res 15 (2013) 1874.
[24] J. Shi, H. Zhang, L. Wang, L. Li, H. Wang, Z. Wang, et al., PEI-derivatized fullerene drug delivery using folate as a homing device targeting to tumor, Biomaterials 34 (2013) 251–261.
[25] P.L. Mccormack, Ferumoxytol. Drugs 72 (2013) 2013–2022.
[26] N. Birta, N. Doca, G. Vlase, T. Vlase, Kinetic of Sorbitol Decomposition Under Non-Isothermal Conditions, J Therm Anal Calorim 92 (2008) 635–638.
[27] K. Anastasakis, a.B. Ross, J.M. Jones, Pyrolysis behaviour of the main carbohydrates of brown macro-algae, Fuel 90 (2011) 598–607.
[28] L. Kastl, D. Sasse, V. Wulf, R. Hartmann, J. Mircheski, C. Ranke, et al., Multiple internalization pathways of polyelectrolyte multilayer capsules into mammalian cells, ACS Nano 7 (2013) 6605–6618.
[29] U. Himmelreich, T. Dresselaers, Cell labeling and tracking for experimental models using magnetic resonance imaging, Methods 48 (2009) 112–124.

Supplementary Information

Polyelectrolyte coating of ferumoxytol nanoparticles for labeling of dendritic cells

Nehar Celikkin, Lucie Jakubcová, Martin Zenke, Mareike Hoss, John Erik Wong, Thomas Hieronymus

Figure S1. DLS scans showing hydrodynamic size distributions of PE-coated and uncoated ferumoxytol MNPs. (A) 6 mg ferumoxytol coated with low MW PDADMAC (1 g/L), (B) 9 mg ferumoxytol coated with low MW PDADMAC (1 g/L), (C) 9 mg ferumoxytol coated with low MW PDADMAC (2 g/L), (D) 12 mg ferumoxytol coated with low MW PDADMAC (2 g/L), (E) 9 mg ferumoxytol coated with high MW PDADMAC (1 g/L), (F) 12 mg ferumoxytol coated with high MW PDADMAC (1 g/L), (G) 3 mg ferumoxytol coated with low MW PEI (1 g/L), (H) 3 mg ferumoxytol coated with high MW PEI (1 g/L) and (I) ferumoxytol.

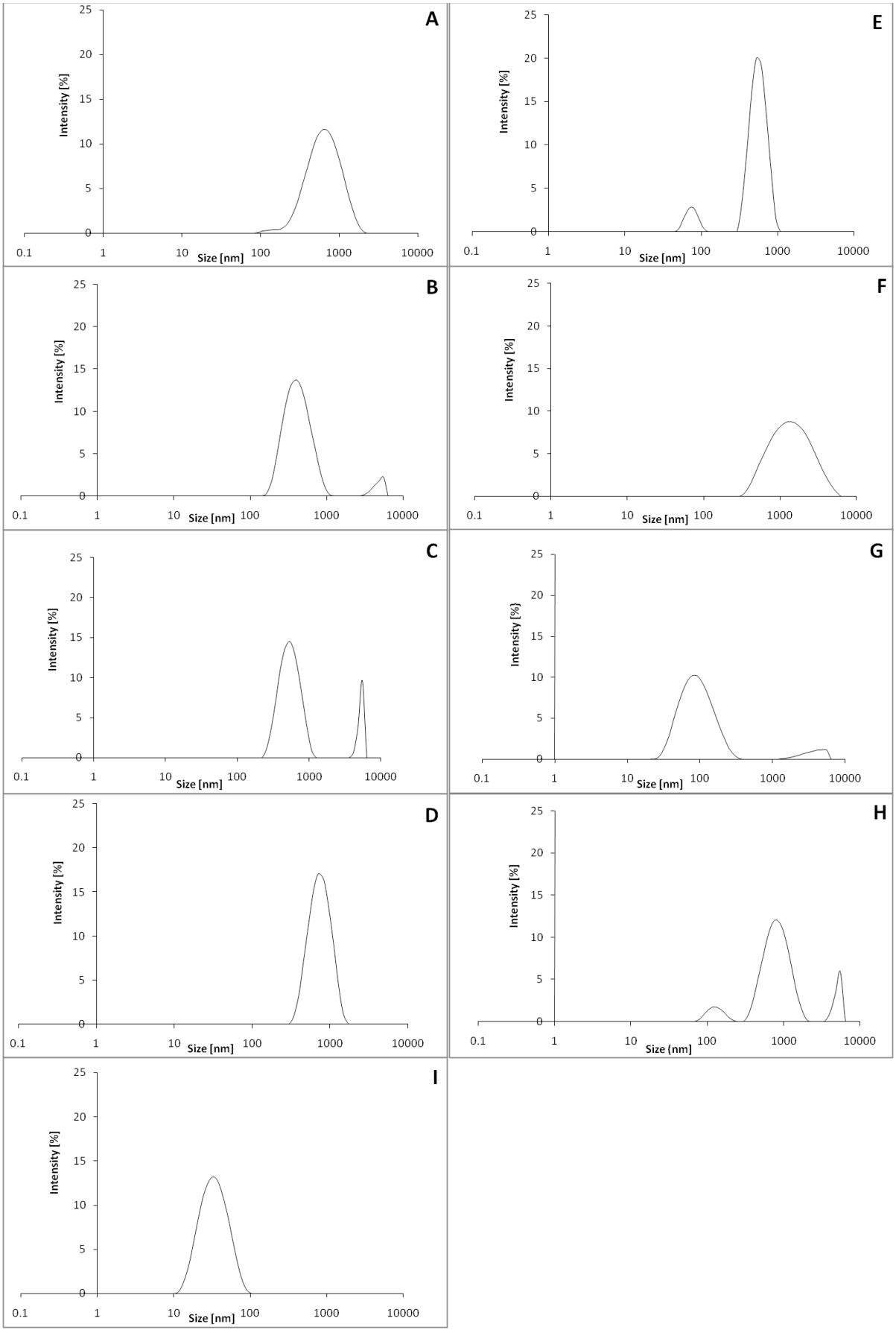

Figure S1. DLS scans of PE-coated and uncoated ferumoxytol MNPs.